Robust electric dipole transition at microwave frequencies for nuclear spin qubits in silicon

Guilherme Tosi,[1,*] Fahd A. Mohiyaddin,[1,†] Stefanie Tenberg,[1] Arne Laucht,[1] and Andrea Morello[1,‡]

[1] *Centre for Quantum Computation and Communication Technology, School of Electrical Engineering & Telecommunications, UNSW Sydney, New South Wales 2052, Australia.*

(Dated: September 21, 2017)

The nuclear spin state of a phosphorus donor (^{31}P) in isotopically enriched silicon-28 is an excellent host to store quantum information in the solid state. The spin's insensitivity to electric fields yield a solid-state qubit with record coherence times, but also renders coupling to other quantum systems very challenging. Here we show that, by coupling the phosphorus donor to an electron shared with an interface dot, a magnetic drive at microwave frequencies creates a strong electric dipole (> 50 Debye) transition for the donor nuclear spin. The magnetic drive also stabilizes the spin's phase and electric dipole, thereby suppressing decoherence arising from electrical noise. The nuclear spin can then be strongly coupled to microwave resonators, with a vacuum Rabi splitting of order 1 MHz, or to other nuclear spins, nearly half a micrometer apart, via strong electric dipole-dipole interaction. This work brings the ^{31}P nuclear qubit into the realm of hybrid quantum systems and opens up new avenues in quantum information processing.

Introduction.—The nuclear spin of a phosphorus donor in silicon has long been the subject of much study in the context of solid-state quantum information processing, either as a qubit cell for large-scale quantum processors [1–3], or a memory for idle quantum information storage [4, 5]. Whether in ensemble form [6] or as individual qubit [7], the ^{31}P nuclear spin has record-long coherence times, thanks to its insensitivity to electric fields and the magnetic noise-free environment of isotopically pure ^{28}Si [8]. However, it cannot trivially be coupled to other quantum systems, and therefore all quantum computing proposals so far impose short interaction distances and slow quantum gate operations [1–3].

In the hybrid approach to quantum information processing [9], different quantum systems interact in a large architecture that benefits from the best properties of each system, which are often coupled together via microwave resonators. In order to couple to individual spin qubits, the resonator vacuum field can be enhanced by shrinking its dimensions in the vicinity of the spin qubit, thereby enhancing the spin-photon coupling rate [10–13]. However, having a Zeeman splitting in the radio-frequency range and a null electric dipole, phosphorus nuclear-spins do not interact naturally with microwave resonators.

The artificial creation of electric dipole transitions has been proposed for different spin systems [14–18] as a way to facilitate scalability. The challenge here is how to make the spin drivable by electric fields without making it too susceptible to electrical noise, which can be strong in nanoscale devices. In this Letter, we show that a strong electric-dipole transition at microwave frequencies can be artificially engineered for the nuclear spin, in the presence of an oscillating magnetic field. This is achieved by sharing an electron between the donor and a quantum dot defined at the Si/SiO_2 interface [18–20]. While the admixture of spin and charge states can potentially make the system very sensitive to electric noise, we show that the nuclear spin phase and electric dipole strength can be stabilized to first-order. By providing a robust coupling between the nuclear spin and electric fields, our scheme opens up new avenues couple to ^{31}P qubits to other quantum systems, including microwave resonators, superconducting qubits and other nuclear spins.

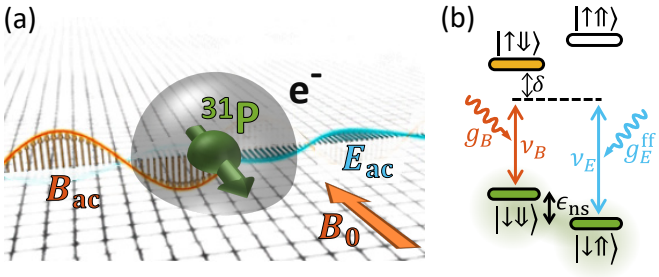

FIG. 1. (a), Spatial schematic view and, (b), energy level diagram for Raman-drive of a Si:P nuclear-spin. ↑ (↓) represents electron spin up (down), while ⇑ (⇓) represents nuclear spin up (down).

Second-order Raman drive of a ^{31}P nuclear spin.—The key ingredients of our proposal are illustrated in Fig. 1a. The ^{31}P nuclear spin interacts with a donor-bound electron via the contact hyperfine interaction, represented by the Hamiltonian $\mathcal{H}_A = A\mathbf{S}\cdot\mathbf{I}$, where $\mathbf{S}$ and $\mathbf{I}$ are the electron and nucleus spin operators, respectively, and A is the electron-nuclear hyperfine coupling ($A \approx 117$ MHz in bulk silicon). Further, an applied static magnetic field B_0 splits the spin states via the Zeeman Hamiltonian $\mathcal{H}_{B_0} = B_0(\gamma_e S_z - \gamma_n I_z)$, where $\gamma_e \approx 28$ GHz/T and

* g.tosi@unsw.edu.au
† Present address: Quantum Computing Institute, Oak Ridge National Laboratory, Oak Ridge, TN, USA
‡ a.morello@unsw.edu.au

$\gamma_n \approx 17.2$ MHz/T are the electron and nucleus gyromagnetic ratios, respectively. Fig. 1b shows the spin levels when $\gamma_e B_0 \gg A$, in which case the electron-nuclear eigenstates are the tensor product of the electron ($|\downarrow\rangle$, $|\uparrow\rangle$) and nuclear ($|\Downarrow\rangle$, $|\Uparrow\rangle$) basis states.

The electron and nuclear spins can be driven by microwave [21] and radio frequency [22] magnetic fields, respectively. Furthermore, we have recently proposed [18] a new transition, which we call 'flip-flop' qubit, between the states $|\downarrow\Uparrow\rangle \leftrightarrow |\uparrow\Downarrow\rangle$. An electric field $E_{\rm ac}$ oscillating at microwave frequency $\nu_E \approx (\gamma_e + \gamma_n)B_0$ is used to shift the electron wavefunction and therefore modulate the hyperfine coupling, $A_{\rm ac}\cos(2\pi\nu_E t)$. Since $\mathcal{H}_A$ is a transverse term in the flip-flop subspace, this results in driving the flip-flop transition at a rate (half Rabi frequency) $g_E^{\rm ff} = A_{\rm ac}/4$.

Now we show how the flip-flop transition provides a way of controlling the nuclear-spin state purely with microwave fields. The key idea is to combine the electrical flip-flop drive with an additional magnetic drive $B_{\rm ac}\cos(2\pi\nu_B t)$, perpendicular to the static B_0 (Fig 1a), that couples the electron spin states $|\downarrow\Downarrow\rangle$ and $|\uparrow\Downarrow\rangle$ at a rate $g_B = \gamma_e B_{\rm ac}/4$. This results in a process analogous to a Raman transition [23], as shown in Fig. 1b: with the electron in the ground spin state $|\downarrow\rangle$, the AC electric and magnetic fields drive the nuclear-spin "up", $|\downarrow\Uparrow\rangle$, and "down", $|\downarrow\Downarrow\rangle$, states, respectively, to a virtual level detuned from the $|\uparrow\Downarrow\rangle$ state by $\delta \gg g_B, g_E^{\rm ff}$. As a result, the nuclear spin is driven via a second order process, with minimal excitation of the electron spin, at a rate:

$$g_E^{\rm ns} = g_B g_E^{\rm ff}/\delta \tag{1}$$

This is equivalent to saying that a microwave magnetic drive $B_{\rm ac}$ creates an electric dipole transition for the nuclear spin with strength $g_E^{\rm ns}/E_{\rm ac}$. Quantitatively, g_B can reach a few MHz [21], and therefore the nuclear spin can be driven at Rabi frequencies close to 1 MHz if the hyperfine interaction can be AC-driven at a few MHz rate. However, if the electron is confined at the donor Coulomb potential, A is quite insensitive to electric fields. Taking the value $\partial A/\partial E \approx 0.5$ Hz V^{-1} m from a recent experiment [24], the corresponding Raman-enabled nuclear electric dipole transition would be only ≈ 5 μDebye (assuming $\delta = 10 g_B$).

Strong electric dipole transition of a ^{31}P nuclear spin.— To increase the nuclear spin electric dipole transition strength, the dependence of A on electric fields can be enhanced by sharing the electron wavefunction with a nearby, tunnel-coupled, interface quantum dot [18] (Fig. 2a). In this case, the electron position can be treated as a two-level charge qubit, represented by the orbital Hamiltonian $\mathcal{H}_{\rm orb} = V_t\sigma_x/2 - (eE_{\rm dc}d/2h)\,\sigma_z$, where V_t is the tunnel coupling between the donor, $|d\rangle$, and the interface-dot, $|i\rangle$, states (Fig. 2a), which are detuned by a static vertical electric field $E_{\rm dc}$ and separated by a distance d; e is the electron charge and h the Planck constant. The resulting electron ground $|g\rangle$ and excited $|e\rangle$ charge eigenstates have an energy difference given by:

$$\epsilon_{\rm o} = \sqrt{(V_t)^2 + (eE_{\rm dc}d/h)^2} \tag{2}$$

Accordingly, the hyperfine coupling operator depends on the electron position, $\mathcal{H}_A^{\rm orb} = A\,(1-\sigma_z)/2\ \mathbf{S}\cdot\mathbf{I}$, which implies a coupling $g_{\rm so}$ between the flip-flop and charge qubits:

$$g_{\rm so} = \frac{A}{4}\frac{V_t}{\epsilon_{\rm o}} \tag{3}$$

Fig. 2b shows the level diagram for a nuclear spin Raman transition taking the electron charge levels into account. Upon application of an AC electric field, $E_{\rm ac}\cos(2\pi\nu_E t)$, the charge levels $|g\rangle$ and $|e\rangle$ are coupled at a rate:

$$g_E = \frac{eE_{\rm ac}d}{4h}\frac{V_t}{\epsilon_{\rm o}}, \tag{4}$$

If $\delta_{\rm so} \gg g_{\rm so}$, $|e\rangle$ is minimally excited while A is still strongly sensitive to electric fields, with $\partial A/\partial E \approx 10^4$ Hz V^{-1} m for V_t on the order of 10 GHz [18]. In this case, $g_E^{\rm ff} \approx g_E g_{\rm so}(1/\delta_E + 1/\delta_{\rm so})/2$, which corresponds to a strong electric-dipole flip-flop transition (~ 40 Debye, assuming $\delta_{\rm so} = 10 g_{\rm so}$). While this enables a strong electric dipole transition for the nuclear spin (~ 4 Debye, assuming $\delta = 10 g_B$ in Eq. 1), this regime makes the nuclear spin transition frequency $\epsilon_{\rm ns}(A) = \gamma_n B_0 + \langle A\rangle/2$ very sensitive to electrical noise, since $\langle A\rangle/2$ is most sensitive at the ionization point, causing fast dephasing.

Robust electric dipole transition of a Si:P nuclear spin.— We now show that the nuclear spin can be made insensitive to electrical noise, while having its electric dipole transition increased even further, by making $\delta_{B,E,{\rm so}} \approx 0$. In this regime, second-order perturbation theory can not be directly applied. We therefore analyze the nuclear spin Hamiltonian by first making it time-independent. After adding the magnetic drive, $\mathcal{H}_{\rm ESR} = B_{\rm ac}\cos(2\pi\nu_B t)(\gamma_e S_z - \gamma_n I_z)$, the total Hamiltonian, $\mathcal{H}_{\rm ns} = \mathcal{H}_{B_0} + \mathcal{H}_A^{\rm orb} + \mathcal{H}_{\rm orb} + \mathcal{H}_{\rm ESR}$, can be expressed in the rotating frame of the magnetic drive by using the transformation: $\mathcal{H}'_{\rm ns} = U^\dagger \mathcal{H}_{\rm ns} U - i\hbar U\dot{U}^\dagger$, with $U = e^{i2\pi\nu_B t(S_z + I_z)}$. After dropping counter-rotating terms, the transformed Hamiltonian becomes time-independent:

$$\mathcal{H}'_{\rm ns} = \delta_B S_z - (\gamma_n B_0 + \nu_B) I_z + \frac{B_{ac}}{2}(\gamma_e S_x - \gamma_n I_x) + \mathcal{H}_{\rm orb} + \mathcal{H}_A^{\rm orb}, \tag{5}$$

where $\delta_B = \gamma_e B_0 - \nu_B$. The dominant energy scale in the above Hamiltonian is given by the term $-(\gamma_n B_0 + \nu_B) I_z$, which represents the nuclear-spin transition, shifted to microwave frequencies in the rotating

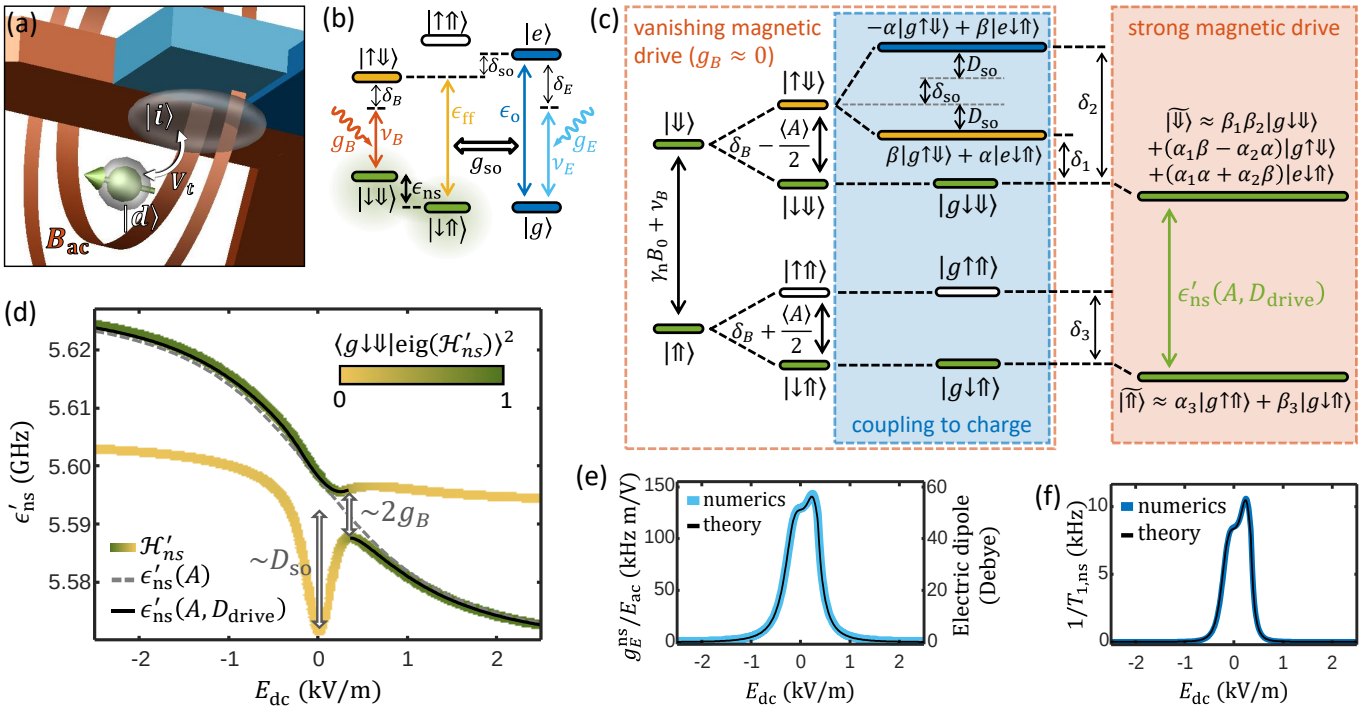

FIG. 2. (a), Components of a Raman-enabled Si:P nuclear electric dipole transition. The electron wavefunction (transparent gray) is shared between an interface-dot, $|i\rangle$, and a donor-bound state, $|d\rangle$, which are coupled by a tunnel rate V_t. Blue gates on top control the electron charge state, and can also communicate the vacuum field of a microwave resonator. A nearby broadband antenna [25] provides the magnetic drive B_{ac}. (b), Bare level diagram in the laboratory frame and, (c), diagonalized basis in the rotating frame, for Raman drive of a nuclear spin via a charge qubit. The effects of the electron spin, charge and magnetic drive are also shown. (d), Nuclear spin transition frequency ϵ'_{ns} in the rotating frame of the magnetic drive B_{ac}, as a function of the static vertical electric field across the donor-dot system, for vanishing magnetic drive ($\epsilon'_{\mathrm{ns}}(A)$ – Eq. 6) and strong magnetic drive ($\epsilon'_{\mathrm{ns}}(A, D_{\mathrm{drive}})$ – Eq. 7). We have assumed $B_0 = 0.2$ T, $V_t \approx \nu_B \approx \gamma_e B_0 + A/4$, $B_{\mathrm{ac}} = 0.6$ mT and $d = 15$ nm. Green/yellow lines show transition frequencies calculated numerically from the Hamiltonian in Eq. 5. The color indicates the amount of bare $|g\downarrow\Downarrow\rangle$ state in the higher $\mathcal{H}'_{ns}$ eigenstate corresponding to each transition. The nuclear spin transition (predominantly $|g\downarrow\Uparrow\rangle \leftrightarrow |g\downarrow\Downarrow\rangle$) anticrosses a flip-flop transition (predominantly $|g\downarrow\Uparrow\rangle \leftrightarrow |g\uparrow\Downarrow\rangle$) at $E_{\mathrm{dc}} = 350$ V/m, with a splitting $\sim 2g_B$. The flip-flop transition is strongly shifted by D_{so} [26], due to its coupling to the charge qubit states around $E_{\mathrm{dc}} = 0$. At $E_{\mathrm{dc}} = 250$ V/m, the nuclear-spin excited eigenstate has $\sim 75\%$ of $|g\downarrow\Downarrow\rangle$ and is robust against electrical noise ($\partial\epsilon'_{\mathrm{ns}}/\partial E_{\mathrm{dc}} = 0$). (e), Nuclear electric dipole strength according to Eqs. 8 (theory) or $\mathcal{H}'_{ns}$ under E_{ac} drive (numerics). It peaks at $E_{\mathrm{dc}} = 250$ V/m. (f). Nuclear-spin relaxation, under magnetic drive, due to coupling to phonons via charge states, Eq. 9

frame (left-most levels in Fig. 2c). These are further split by the electron spin Hamiltonian, $(\delta_B + \langle A\rangle I_z)\, S_z + 2g_B S_x$ (where the hyperfine coupling value, $\langle A\rangle$, depends on the electron charge state), yielding the electron-nuclear spin levels shown in Fig. 2c, depicted in the limit of vanishing B_{ac} (and therefore g_B). In this case, the nuclear-spin transition frequency, in the rotating frame, with the electron in the ground state, is:

$$\epsilon'_{\mathrm{ns}}(A) = \gamma_n B_0 + \nu_B + \langle A\rangle/2. \tag{6}$$

This dependence is plotted as a dashed line in Fig. 2d, and is valid when the electron charge states are far detuned from the spin levels ($\delta_{\mathrm{so}} \gg g_{\mathrm{so}}$), as discussed in the last section. The plot highlights the strong depence of ϵ'_{ns} on electric fields.

However, the nuclear spin dispersion changes dramatically when δ_{so} approaches zero. There, $\mathcal{H}_A^{\mathrm{orb}}$ hybridizes the flip-flop and charge states, as shown in Fig. 2c, with coefficients α and β given in [26]. Furthermore, by increasing the magnetic drive amplitude B_{ac}, the Hamiltonian term $2g_B S_x$ couples the electron spin $\uparrow$ and $\downarrow$ states, hybridizing the system eigenstates. Two of those eigenstates, which we call $|\widetilde{\Downarrow}\rangle$ and $|\widetilde{\Uparrow}\rangle$ (Fig. 2c), are chiefly composed of the tensor product of the nuclear $|\Downarrow\rangle$, $|\Uparrow\rangle$ states with the ground charge state $|g\rangle$ and the ground $|\downarrow\rangle$ electron spin state. The energy splitting between $|\widetilde{\Downarrow}\rangle$ and $|\widetilde{\Uparrow}\rangle$, ϵ'_{ns}, equals the bare nuclear-spin transition, $\epsilon'_{\mathrm{ns}}(A)$ (Eq. 6), plus an amount that dependents on E_{dc}:

$$\epsilon'_{\mathrm{ns}}(A, D_{\mathrm{drive}}) = \epsilon'_{\mathrm{ns}}(A) - D_{\mathrm{drive}}(E_{\mathrm{dc}}), \tag{7}$$

where D_{drive} corresponds to an AC-Stark shift, quantitavely defined in [26]. This equation agrees with numerical simulations of the full Hamiltonian of Eq. 5 (Fig. 2d). In particular, around the ionization point, the flip-

flop transition, strongly shifted due to its coupling to the charge state, anticrosses the nuclear spin transition, creating a region where $\partial\epsilon'_{\rm ns}/\partial E_{\rm dc} = 0$, i.e. a first-order 'clock transition' [27, 28] where $\epsilon'_{\rm ns}$ is insensitive to electric noise. Further adjustment of the parameters allows for $\partial^2\epsilon'_{\rm ns}/\partial {E_{\rm dc}}^2 = 0$ (second-order clock transition), improving noise insensitivity even further. Assuming a realistic 100 V/m r.m.s. quasi-static noise amplitude (equivalent to a 1.5 μeV charge detuning noise for $d = 15$ nm, consistent with measured values [29]), the predicted nuclear spin dephasing rate is only $\sim$ 1-10 kHz. Note that, similarly to dressed states [30–32], the addition of the magnetic drive prolongs the coherence of our qubit. However, here the suppresed noise is of electrical nature (despite the drive being magnetic), given the particular hybridization with charge states.

In a key result of our proposal, the small admixture of the excited charge state, $|e\rangle$, into $\widetilde{|\Downarrow\rangle}$ creates an electric-dipole transition for the nuclear spin. Indeed, the $\widetilde{|\Downarrow\rangle} \leftrightarrow \widetilde{|\Uparrow\rangle}$ transition can be electrically-driven at a rate given by the charge admixture coefficients in Fig. 2c,

$$g_E^{\rm ns} = g_E \beta_3 \left(\alpha_1 \alpha + \alpha_2 \beta\right), \tag{8}$$

where the exact form of α_1, α_2 and β_3 is given in [26]. This electric dipole transition, at microwave frequencies, can reach > 50 Debye around $E_{\rm dc} = 0$ (Fig. 2e). This means that even an extremely weak AC electric field, $E_{\rm ac} \approx 3$ V/m, can drive a nuclear spin transition at a MHz Rabi frequency. This is two orders of magnitude faster than the typical Rabi frequencies obtained with standard (NMR) magnetic drive at radiofrequency [22], and an order of magnitude faster than obtained (at very high electric drive amplitudes) in a recent experiment where electrically-driven NMR was achieved by modulating the quantization axis of the electron spin [33]. Note that, although we assumed $\delta_{\rm so} \to 0$, the electric and magnetic driving fields are still off-resonance with the eigenstates of the full Hamiltonian (hybridized charge-flip-flop states [26]), ensuring minimal excitation of the $|\uparrow\rangle$ and $|e\rangle$ states.

This strong electric dipole at microwave frequencies provides a pathway for strong coupling a ^{31}P nuclear spin to microwave resonators [34], where a vacuum field $E_{\rm vac}$ of a few V/m can result in vacuum Rabi splittings around 1 MHz. This could be achieved e.g. by connecting the top blue gate on Fig. 1a to the center pin of a superconducting coplanar waveguide resonator. Similarly to other proposals [35–38], here it is a classical drive ($B_{\rm ac}$) that enables coupling to a quantum field ($E_{\rm vac}$).

Importantly, at the same bias point where the 'clock transition' ($\partial\epsilon'_{\rm ns}/\partial E_{\rm dc} = 0$) for the nuclear energy takes place, the nuclear electric dipole is also first-order insensitive to electrical noise, since $\partial g_E^{\rm ns}/\partial E_{\rm dc} = 0$ (Fig. 2e). A realistic 1.5 μeV charge detuning noise [29]) would make $g_E^{\rm ns}$ fluctuate by only $\sim 2\%$.

The engineered nuclear electric dipole also opens up

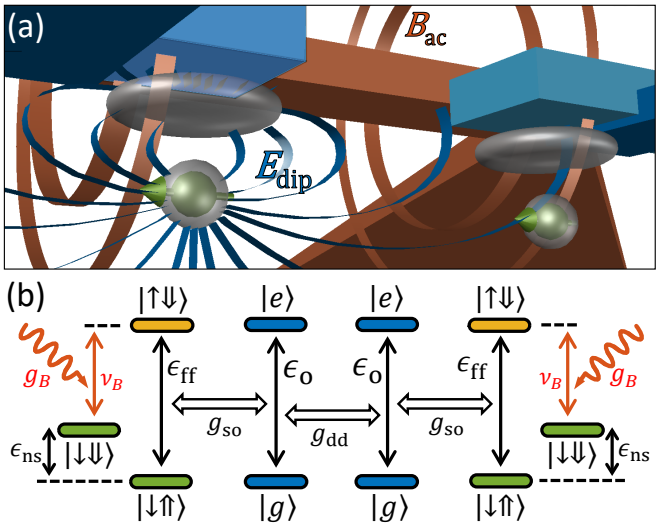

FIG. 3. (a), Components, and (b), level diagram, for long-distance coupling of two Si:P nuclear-spins via electric dipole-dipole interactions. Each displaced electron produces an electric dipole field $E_{\rm dip}$ (shown only for one electron).

a new pathway for nuclear spin relaxation: $\widetilde{|\Downarrow\rangle}$ can decay into $\widetilde{|\Uparrow\rangle}$ through a peculiar effect, where a photon from the driving field is combined with the nuclear spin energy (which is at radiofrequency) to emit a phonon at microwave frequency. The rate for this process can be roughly estimated as the admixture of the $|e\rangle$ charge excited state into the $\widetilde{|\Downarrow\rangle}$ eigenstate times the charge relaxation rate $1/T_{1,\rm o}$:

$$1/T_{1,\rm ns} = \widetilde{\langle\Downarrow|e\rangle}\langle e|\widetilde{\Downarrow\rangle}/T_{1,\rm o} \approx |\alpha_1\alpha + \alpha_2\beta|^2/T_{1,\rm o}, \tag{9}$$

where $1/T_{1,\rm o} = \Theta\epsilon_{\rm o}{V_t}^2$, [39] with $\Theta \approx 2.37 \times 10^{-24}$ s^2 determined by the silicon crystal properties.

As Fig. 2f shows, $1/T_{1,\rm ns}$ peaks, around the ionization point, at a value that is still two orders of magnitude slower than e.g. the spin's coupling rate to a microwave resonator, therefore allowing the strong coupling regime to be well within reach.

Long-distance coupling of nuclear spin qubits.— As a further natural extension, nuclear spins can be coupled directly to each other through the electric dipole-dipole interaction that results from displacing the electron charge from the donor (Fig. 3a) [18]. This can be exploited to couple a nuclear spin to the electric dipole transition of another nuclear spin.

The interaction energy between two charge dipoles, $e\mathbf{d}_1$ and $e\mathbf{d}_2$, separated by $\mathbf{r}$, is:

$$V_{\rm dip} = \frac{e^2}{4\pi\varepsilon_0\varepsilon_r}\frac{\mathbf{d}_1\cdot\mathbf{d}_2 - 3(\mathbf{d}_1\cdot\mathbf{r})(\mathbf{d}_2\cdot\mathbf{r})/r^2}{r^3}, \tag{10}$$

where ε_0 is the vacuum permittivity and ε_r the material's dielectric constant ($\varepsilon_r = 11.7$ in silicon). With

the charge dipole of each donor-interface state being $ed_i(1+\sigma_{z,i})/2$, this dipole-dipole interaction is equivalent to a coupling term between the charge qubits (Fig. 3b) equal to $g_{\rm dd} = (V_{\rm dip}V_{t,1}V_{t,2})/(4\epsilon_{{\rm o},1}\epsilon_{{\rm o},2})$ [18].

Two distant nuclear spin qubits can then be coupled when both electrons are around their ionization point and an AC magnetic drive $B_{\rm ac}$ is applied (Fig. 3a,b). For the operation parameters used in Fig. 2, $\epsilon_{\rm o} \approx \epsilon_{\rm ff} \approx \nu_B + \epsilon_{\rm ns}$ and $g_B \ll g_{\rm so}$, the two-qubit coupling rate is found, via second-order perturbation theory, to be:

$$g_{\rm 2q}^{\rm ns} = \left(\frac{g_B}{g_{\rm so}}\right)^2 g_{\rm dd}, \tag{11}$$

which is valid if $g_B \ll (g_{\rm so})^2/g_{\rm dd}$. For two nuclear spins $r = 0.4$ μm apart, $g_{\rm 2q}^{\rm ns} = 0.55$ MHz, yielding a $\sqrt{i\rm SWAP}$ gate time of ~ 230 ns. This is a tremendous improvement over Kane's proposal [1], for which an exchange-mediated $\sqrt{i\rm SWAP}$ gate between two ^{31}P nuclear spins $r = 15$ nm apart takes 3 μs.

Conclusion.—Until now, quantum computer architectures that aimed at encoding information in the ^{31}P nuclear spin [1–3] had to be built around a qubit with an extremely small magnetic dipole, that only responds to radiofrequency signals. By engineering an electric dipole transition, we have shown here that the ^{31}P qubit can also be driven at microwave frequencies, and coupled to other nuclei or to microwave cavities via electric dipole interactions. The effects of electrical noise can be strongy suppressed by operating around 'clock transitions', thus preserving the excellent quantum coherence properties of the ^{31}P system. The nuclear spin can then be incorporated into hybrid quantum architectures [9], where it can be used *e.g.* as a long-lived quantum memory [5], or placed in large arrays of electric-dipole coupled nuclear qubits.

ACKNOWLEDGMENTS

We thank A. Pályi for insightful comments. This research was funded by the Australian Research Council Centre of Excellence for Quantum Computation and Communication Technology (project number CE110001027), the US Army Research Office (W911NF-13-1-0024) and the Commonwealth Bank of Australia.

[1] B. E. Kane, *Nature* **393**, 133 (1998)
[2] J. O'Gorman *et al.*, *NPJ Quantum Information* **2**, 15019 (2016)
[3] C. D. Hill *et al.*, *Science Advances* **1**, e1500707 (2015)
[4] J. J. L. Morton *et al.*, *Nature* **455**, 1085 (2008)
[5] S. Freer *et al.*, *Quantum Science and Technology* **2**, 015009 (2017)
[6] K. Saeedi *et al.*, *Science* **342**, 830 (2013)
[7] J. T. Muhonen *et al.*, *Nature Nanotech.* **9**, 986 (2014)
[8] K. M. Itoh, and H. Watanabe, *MRS Communications* **4**, 143 (2014)
[9] Z.-L. Xiang *et al.*, *Rev. Mod. Phys.* **85**, 623 (2013)
[10] G. Tosi *et al.*, *AIP Advances* **4**, 087122 (2014)
[11] M. D. Jenkins *et al.*, *Dalton Trans.* **45**, 16682 (2016)
[12] P. Haikka *et al.*, *Phys. Rev. A* **95**, 022306 (2017)
[13] B. Sarabi, P. Huang, and N. M. Zimmerman, *arXiv*:1702.02210 (2017)
[14] M. Pioro-Ladriere *et al.*, *Nature Phys.* **4**, 776 (2008)
[15] Z. Shi *et al.*, *Phys. Rev. Lett.* **108**, 140503 (2012)
[16] M. Russ, and G. Burkard, *arXiv*:1611.09106 (2016)
[17] J. Salfi *et al.*, *Phys. Rev. Lett.* **116**, 246801 (2016)
[18] G. Tosi *et al.*, *Nature Comms.* **8**, 450 (2017)
[19] M. J. Calderón *et al.*, *Phys. Rev. Lett.* **96**, 096802 (2006)
[20] M. Veldhorst *et al.*, *Nature Nanotech.* **9**, 981 (2014)
[21] J. J. Pla *et al.*, *Nature* **489**, 541 (2012)
[22] J. J. Pla *et al.*, *Nature* **496**, 334 (2013)
[23] P. Kok, and B. Lovett, *Introduction to Optical Quantum Information Processing* (Cambridge University Press, 2010) pp. 219–222
[24] A. Laucht *et al.*, *Science Advances* **1**, e1500022 (2015)
[25] J. P. Dehollain *et al.*, *Nanotechnology* **24**, 015202 (2013)
[26] See Supplemental Material at [URL will be inserted by publisher] for a note on electron g-factors, and the full expressions of the systems eigenstates and energy shifts.
[27] J. Bollinger *et al.*, *Phys. Rev. Lett.* **54**, 1000 (1985)
[28] G. Wolfowicz *et al.*, *Nature Nanotech.* **8**, 561 (2013)
[29] B. M. Freeman, J. S. Schoenfield, and H. Jiang, *Appl. Phys. Lett.* **108**, 253108 (2016)
[30] P. London *et al.*, *Phys. Rev. Lett.* **111**, 067601 (2013)
[31] A. Laucht *et al.*, *Phys. Rev. B* **94**, 161302 (2016)
[32] A. Laucht *et al.*, *Nature Nanotech.* **12**, 61 (2017)
[33] A. Sigillito *et al.*, *Nature Nanotech.* (2017)
[34] A. Blais *et al.*, *Phys. Rev. A* **69**, 062320 (2004)
[35] J. Pachos, and H. Walther, *Phys. Rev. Lett.* **89**, 187903 (2002)
[36] L. Childress, A. S. Sørensen, and M. D. Lukin, *Phys. Rev. A* **69**, 042302 (2004)
[37] Z.-B. Feng, *Phys. Rev. A* **78**, 032325 (2008)
[38] M. Abanto *et al.*, *Phys. Rev. B* **81**, 085325 (2010)
[39] P. Boross, G. Széchenyi and A. Pályi, *Nanotechnology* **27**, 314002 (2016)